Impact of Variable viscosity, Non-linear thermal radiation and irregular heat sources on non-Darcy hydromagnetic convective heat transfer flow past a stretching surface filled with Al_2O_3-water nanofluid

Dr. B. Sreenivasa Reddy[1] and A.Malleswari[2]
Associate Professor, Department of Applied Mathematics, Yogivemana University, Kadapa, A.P., India, Email : keerthireddybsr@gmail.com
Research Scholar, Department of Applied Mathematics, Yogivemana University, Kadapa, A.P., India, Email :andelamalleswari123@gmail.com

Abstract :

We analyze the combined influence of nonlinear convective and irregular heat sources on non-Darcy convective heat transfer flow of Al_2O_3-water nanofluid past a stretching sheet with variable properties. Using similarity variables the non-linear partial differential equationsare converted into ordinary differentialequations and are solved by using Finite-element method with quadratic shape functions.From this analysis, it is observed that primary velocity, temperature enhance, secondary velocity with viscosity parameter(B).Nu grows decays for higher values of viscosity parameter. Higher the strength of the space/temperature(A11/B11) dependent heat source leads to a depreciation in the flow variables.

Keywords : Al_2O_3-water nanofluid; Stretching Sheet,non-linear thermal radiation, Finite Element Method,irregular heat sources.

1.INTRODUCTION:

The study of nonlinear thermal radiative fluid flow passing over a stretched surface is an area of potential interest for the researchers due to its applications in many engineering and physical processes. Some applicable areas of such processes are solar power technology, nuclear plants, aircraft, propulsion devices, combustion chambers and chemical processes at high operating temperature. Particularly, the thermal radiation effect plays a vital role in controlling the heat transfer process at polymer processing industry. In view of this, Mushtaq et al. [21], Pantokratoras and Fang [26], Shehzad et al. [30]were first to study the effect of nonlinear thermal radiation on the Sakiadis flow and Maxwell fluid. They employed the numerical method to solve the nonlinear thermal radiation problem, three-dimensional flow of Jeffrey fluid over stretched surface and developed the series solutions to analyze the results. Cortell [7] discussed the influence of thermal radiation effect on heat flow over a stretching sheet. The investigations by Hussain et al. [12], Animasaum et al. [3], Krupalakshmi et al. [17] and Mahanthesh et al. [19] dealt with the flows under nonlinear radiation effect and different physical conditions.

In modern engineering and technology, the consumption of energy resources has become a prime interest due to its progressive significance in industrial systems. However, it is commonly noticed that due to environmental pollution and global warming issue, the whole world is facing the challenges of energy crises. The study of nanofluid, originated by Choi [6] in 1995, attracted a good deal of attention in recent years. The nanofluids are considered as the most potential coolants in mechanical industries and engineering systems. The nano materials are specified as metallic thermophysical parameters engrossed in the base liquid and subsequently enhanced the weaker thermal properties of that base material. Several efforts have been carried out to examine the anomalous characteristics feature of nanoparticles. For instance, Buongiorno [5] studied the two important slip mechanisms, namely thermophoresis and Brownian aspects, in the enhancement of convective heat transfer. The flow of nanofluid by using Buongiorno model over a stretching surface is presented by Khan and Pop [16]. Bhatti et al. [4] explored the thermo diffusion and Brownian

effects in the flow of tangent hyperbolic nanofluid submerged in the porous medium. Sheikholeslami et al. [31] utilized the Fe_3O_4 nanoparticles in the base fluid and proved that the thermal conductivity of the base liquid can be proficiently enhanced with the utilization of these nanoparticles. Khan et al. [14, 15], Rashidi et al. [26], Mabood et al[18]have explored the three-dimensional flow of water-based nanofluid under the influence of thermal radiation. Hayat et al [11] and Wakif et al. [36,37] have been described MHD three-dimensional flow of visco-elastic nanofluid in the presence of nonlinear thermal radiation.Prabavathi et al [25] have discussed three-dimensional heat and mass transfer flow over a stretching sheet filled with Al_2O_3-water based nanofluid with heat generation/absorption.

In most of the studies, the viscosity of the fluid was assumed to be constant. When the effects of variable viscosity is taken into account, the flow characteristics are significantly changed compared to the constant property case. Convection flow in nature and engineering phenomena requires that viscosity and thermal conductivity of fluids vary with temperature. For instance, the viscosity of dry air at 100^0 C is $21.94x10^{-6}$ kg/ms while at 200^0C it is $26.94x10^{-6}$ kg/ms. Ali [1] was briefly discussed the effect of variable viscosity on mixed convection heat transfer along a vertical moving surface. Vajravelu et al [35], Singh and Shweta [33] and Isaac and Anselm [13] shoed that, velocity distribution decreases with increase in viscosity while the temperature profiles increase with increase in variable viscosity. Devi and Prakash [9], Animasaun [3],Sreenivasulu et al [34] have examined temperature-dependent viscosity and thermal conductivity effects on hydromagnetic flow over a slandering stretching sheet with heat source/sink. Makinde et al. [20] describes the MHD flow of a variable viscosity nanofluid over a radially stretching convective surface with radiative heat. Aliveni and Sreevani [2] have discussed the effect of variable viscosity, radiation absorption on non-darcy mhd convective heat and mass transfer flow past stretching sheet with non-uniform heat sources. Recently, Satya Narayana and Ramakrishna [28] discussed the effect of Brownian motion and thermophoresis, activation energy on hydromagnetic convective heat transfer flow of nanofluid in a vertical channel. In the being there of heat sources, Nagasasikala [22] has examined the impact of dissipation on convective heat and mass transfer analysis flow nanofluid in a vertical channel. Devasena [8]has talked about how thermal radiation affects the flow of heat in nanofluids having Brownian motion and thermophoresis.

It is worth mentioning that non-Darcial forced flow boundary layers from a very important group of flows, the solution of which is of great importance in many practical application such as in biomechemical problems. In filtration transpiration cooling and geothermal. Singh and Tewani [32] studied the effect of thermal stratification on non-Darcial free convection flow by using from Ergun[10] model to include the inertia effect. It is well known that there exists non-Darcial flow phenomena bodies inertia effect and solid-boundary viscous resistance.

In this paper,an attempt has been made to investigate the impact of nonlinear thermal radiation and irregular heat sources on convective heat transfer flow of Al_2O_3-water nanofluid past bilinear stretching sheet.The transformed boundary layer equations which represent the flow heat and mass transfer are solved numerically using finite element method with quadratic interpolation function.

2. MATHEMATICAL FORMULATION

Consider the steady three dimensional viscous incompressible laminar MHD boundary layer flow of a nanofluid past a stretching sheet through nanofluid-saturated porous medium filled with water – based alumina nanofluid situated at$z = 0$. The coordinate system is chosen such that (u v w) be the velocity components along (xyz) directions respectively.We also consider a constant magnetic field of strengthB_0 in the z - direction. The flow is caused

by the stretching of the sheet which moves in its own plane with the surface velocity *ax* where *a* (stretching rate) is positive constant. The stretching surface is maintained at uniform temperature T_w and these values are assumed to be greater than the ambient temperature T_∞. Under the above assumptions the governing equations describing the momentum and energy in the presence of non-linear thermal radiation and irregular heat sources take the following form:

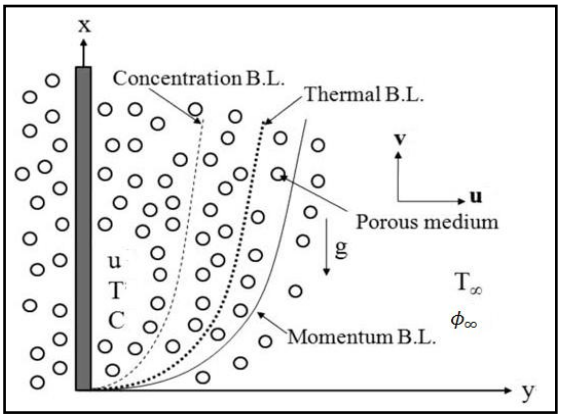

Fig. 1 Physical model and Coordinate system

$$\frac{\partial u}{\partial x}+\frac{\partial v}{\partial y}+\frac{\partial w}{\partial z}=0 \tag{1}$$

$$u\frac{\partial u}{\partial x}+v\frac{\partial u}{\partial y}|+w\frac{\partial u}{\partial z}=\frac{\mu_{nf}}{\rho_{nf}}\frac{\partial^2 u}{\partial z^2}-\frac{\mu_{nf}}{\rho_{nf}}\frac{1}{k}u-\frac{1}{\rho_{nf}}\sigma_{nf}B_o^2u+(\rho\beta)_{nf}(T-T_\infty)-(\frac{\mathrm{Cb}}{\sqrt{k}})\mathrm{u}^2 \tag{2}$$

$$u\frac{\partial v}{\partial x}+v\frac{\partial v}{\partial y}|+w\frac{\partial v}{\partial z}=\frac{\mu_{nf}}{\rho_{nf}}\frac{\partial^2 v}{\partial z^2}-\frac{\mu_{nf}}{\rho_{nf}}\frac{1}{k}v-\frac{1}{\rho_{nf}}\sigma_{nf}B_o^2v-(\frac{\mathrm{Cb}}{\sqrt{k}})\mathrm{v}^2 \tag{3}$$

$$u\frac{\partial T}{\partial x}+v\frac{\partial T}{\partial y}+w\frac{\partial T}{\partial z}=\alpha_{nf}\frac{\partial^2 T}{\partial z^2}-\frac{1}{(\rho C_p)_{nf}}\frac{\partial q_z}{\partial z}+\frac{q'''}{(\rho C_p)_{nf}} \tag{4}$$

The associated boundary conditions are

$$u=ax+\frac{2-\gamma}{\gamma}\lambda\frac{\partial u}{z},v=by+\frac{2-\gamma}{\gamma}\delta\frac{\partial v}{\partial z},w=-U_o,T=T_w at\ z=0$$
$$u\to\infty,v\to 0,T\to T_\infty \qquad as\ z\to\infty \tag{5}$$

The dynamic viscosity of the nanofluids is assumed to be temperature dependent as follows:

$$\mu_f(T)-\mu_o Exp(-m(T-T_o)) \tag{6}$$

where μ_o is the nanofluid viscosity at the ambient temperature To. m is the viscosity variation parameter which depends on the particular fluid.

The dynamic viscosity μ_{nf} density ρ_{nf} thermal diffusivity α_{nf} thermal conductivity $(\rho C_p)_{nf}$ specific heat k_{nf} heat capacitance electric conductivity σ_{nf} of the nanofluid and kinematic viscosity ν_f of the base fluid are defined as follows:

$$\alpha_{nf}=\frac{k_{nf}}{(\rho C_p)_{nf}},\mu_{nf}=\frac{\mu_f}{(1-\phi)}\ \nu_f=\frac{\mu_f}{\rho_f},\rho_{nf}=(1-\phi)\rho_f+\phi\rho_s$$
$$(\rho C_p)_{nf}=(1-\phi)(\rho C_p)_f+\phi(\rho C_p)_s\ (\rho\beta)_{nf}=(1-\varphi)(\rho\beta)_f+\varphi(\rho\beta)_s \tag{7}$$

$$\sigma_{nf}=\sigma_f(1+\frac{3(\sigma-1)\phi}{\sigma+2-(\sigma-1)\phi}),\sigma=\frac{\sigma_s}{\sigma_f}\ k_{nf}=k_f(\frac{k_s+2k_f-2\phi(k_f-k_s)}{k_s+2k_f+2\phi(k_f-k_s)}) \tag{8}$$

The similarity transformations are introduced as

$$\eta = (\sqrt{\frac{a}{\nu_f}})y, u = axf'(\eta), v = byg'(\eta), w = -(\sqrt{(a\nu_f)})(f+g),$$

$$\theta = \frac{T - T_\infty}{T_w - T_\infty} \tag{9}$$

By using Rosseland approximation for radiation the radiative heat flux q_r is defined as

$$q_r = -\frac{4\sigma^* T_\infty^3}{3\beta_R}\frac{\partial T'^4}{\partial z} = -\frac{16\sigma^* T_\infty^3}{3\beta_R}\frac{\partial^2 T}{\partial z^2} \tag{10}$$

The non-dimensional temperature $\theta = \frac{T - T_\infty}{T_w - T_\infty}$ can be simplified as

$$T = T_\infty(1 + (\theta_w - 1)\theta) \tag{11}$$

where $\theta_w = \frac{T_w}{T_\infty}$ is the temperature parameter.

The non-uniform heat source/sink q''' is defined as

$$q''' = \frac{k_f}{\nu_f}[A_{11}(T_w - T_\infty) f' + B_1(T - T_\infty)] \tag{12}$$

Where $A_{11}$and B_1 are the coefficients of space and temperature-dependent heat source/sink respectively. The case $B_1>0$ corresponds to internal heat source and the case $B_1<0$ corresponds to internal heat sink.

Using Eqns. (9) (10) and (11) the governing non-linear partial differential equations (1) - (5) together with the boundary conditions (6) takes the form

$$\left.\begin{aligned} f''' - Bf'\theta' - Kf' + \exp(B\theta)(A_1[(f+g)f'' - (f')^2] - \frac{A_1A_7}{A_2}M^2 f' + \\ + (\frac{GA_1A_8}{A_2})\theta) - (\frac{A_1}{A_2})fs(f')^2 = 0 \end{aligned}\right| \tag{13}$$

$$g''' - Bg'\theta'' + Kg' + \exp(\mathrm{B}\theta)(A_1[(f+g)g'' - (g')^{2]} - \frac{A_1A_7}{A_2}M^2 g') - (\frac{A_1}{A_2})fs(g')^2 = 0 \tag{14}$$

$$\left.\begin{aligned} (1 + \frac{4Rd}{3A_4})\theta'' + \Pr\frac{A_3}{A_4}(f+g)\theta' + \frac{Rd}{A_4}(\theta_w - 1)^3(3\theta^2(\theta')^2 + \theta^3\theta'') + \frac{3Rd}{A_4}((\theta_w - 1)^2 \\ (2\theta^2(\theta')^2 + \theta^2\theta'') + \frac{3Rd}{A_4}((\theta_w - 1)(2\theta^2(\theta')^2 + \theta^2\theta'') + \mathrm{A}_{11}\, f' + B_{11}\theta = 0 \end{aligned}\right| \tag{15}$$

The transformed boundary conditions are

$$\left.\begin{aligned} f'(0) = 1 + B1\, f''(0), g'(0) = \alpha + Rg'(0),\ f(0) + g(0) = V_0, \\ \theta(0) = 1 \quad at\ \ \eta = 0 \\ f' = 0, g' = 0, \theta = 0 \quad as\ \ \eta \to \infty \end{aligned}\right| \tag{16}$$

where prime indicates ordinary differentiation with respect to η. In usual notations

$$\Pr = \frac{\nu_f}{\alpha_f}.M^2 = \frac{\sigma B_o^2}{\rho_f}, Rd = \frac{4\sigma^\bullet T_\infty^3}{\beta_R k_f}, \alpha = \frac{b}{a}, B1 = \frac{2-\gamma_1}{\gamma_1}(\sqrt{\frac{2}{\nu_f}})\lambda_1,$$

$$\mathrm{Gr} = \frac{\beta g a^2(T_w - T_\infty)}{\mu_f^2}, \mathrm{K} = \frac{k}{a^2}, \mathrm{B} = \mathrm{m}(\mathrm{T}_w - \mathrm{T}_\infty), \mathrm{fs} = \frac{Cb}{\sqrt{k}}$$

$$A_{11} = \frac{A'_{11}}{ax}, \mathrm{B}_{11} = \frac{B'_{11}}{ax}, A_1 = (1-\varphi)^{2.5}, A_2 = 1 - \varphi + \varphi(\frac{\rho_s}{\pi_f}),$$

$$A_3 = 1-\phi+\phi(\frac{(\rho C_p)_s}{(\rho C_p)_f}), A_4 = \frac{k_{nf}}{k_f}, A_7 = \frac{\sigma_{nf}}{\sigma_f} = 1+\frac{3(\sigma-1)\phi}{(\sigma+2)-\phi(\sigma+1)}, A_8 = 1-\phi+\phi(\frac{(\rho\beta)_s}{(\rho\beta)_f})$$

Quantities of practical interest in this problem are the local skin-friction coefficient along *x* and *y* directions local Nusselt number. These are defined respectively as

$$C_{f_x} = \frac{f''(0)}{(1-\phi)^{2.5}\,\mathrm{Re}_x^{1/2}},\ C_{fy} = \frac{g''(0)}{(1-\phi)^{2.5}\,\mathrm{Re}_x^{1/2}},\ Nu_x = -(1+R\theta_w)^2\theta'(0)\,\mathrm{Re}_x^{1/2} \qquad (17)$$

Table 1. Thermo - physical properties of water and nanoparticles.

Fluid	$\rho\left(\frac{Kg}{m^3}\right)$	$C_p\left(\frac{J}{kgK}\right)$	$k\left(\frac{W}{mK}\right)$	$\beta\times10^5(K^{-1})$
Pure water	997.1	4179	0.613	21
Copper (Cu)	8933	385	401	1.67
Silver (Ag)	10500	235	429	1.89
Alumina (Al_2O_3)	3970	765	40	0.85
Titanium Oxide (TiO_2)	4250	686.2	8.9538	0.9

3.FINITE ELEMENT ANALYSIS:

The finite element analysis with quadratic polynomial approximation functions is carried out along the axial direction of the wall. The behavior of the velocity temperature profiles has been discussed computationally for different variations in governing parameters. The Galarkin method has been adopted in the variational formulation in each element to obtain the global coupled matrices for the velocity, temperature in course of the finite element analysis.

Choose an arbitrary element f^k and let f^k, g^k, θ^k be the values of f, g,θ, in the element ek

We define the error residuals as

$$E_f^k = f''' - Bf'\theta' + A_1[(f+g)f'' - (f')^2] - Kf' - \frac{A_1A_7}{A_2}M^2f' + (\frac{GA_1A_8}{A_2})\theta - (\frac{A_1}{A_2})fs(f')^2 \quad (18)$$

$$E_g^k = g''' - Bg'\theta' + A_1[(f+g)g'' - (g')^{2]} + Kg' - \frac{A_1A_7}{A_2}M^2g' - (\frac{A_1}{A_2})fs(g')^2 \quad (19)$$

$$E_\theta^k = (1+\frac{4Rd}{3A_4})\theta'' + \Pr\frac{A_3}{A_4}(f+g)\theta' + \frac{Rd}{A_4}(\theta_w-1)^3(3\theta^2(\theta')^2+\theta^3\theta'') + \frac{3Rd}{A_4}((\theta_w-1)^2(2\theta^2(\theta')^2+\theta^2\theta'') + \frac{3Rd}{A_4}((\theta_w-1)(2\theta^2(\theta')^2+\theta^2\theta'') + A_{11}f' + B_{11}\theta \quad (20)$$

where f^k $g^k\theta^k$ are values of f, g, θ in the arbitrary element ek. These are expressed as linear combinations in terms of respective local nodal values.

$$f^k = f_1^k\psi_1^k + f_2^k\psi_1^k + f_3^k\psi_3^k \quad g^k = g_1^k\psi_1^k + g_2^k\psi_1^k + g_3^k\psi_3^k \quad \theta^k = \theta_1^k\psi_1^k + \theta_2^k\psi_2^k + \theta_3^k\psi_3^k$$

where ψ_1^k ψ_2^k --------- etc are Lagrange's quadratic polynomials.

Galerkin's method is used to convert the partial differential Eqs. (18) – (20) into matrix form of equations which results into 3x3 local stiffness matrices. All these local matrices are assembled into a global matrix by substituting the global nodal values of order 1 and using inter element continuity and equilibrium conditions.In solving these global matrices an iteration procedure has been adopted to include the effects of pertinent parametric variations.The iteration process is continued until the desired convergence is gained.

Table 2. Comparison of$-\theta'(0)$ with previously published data.
(A=θw=1,fs=0, A11=0)

Parameter			$-\theta'(0)$	
M	θ_w	R	Hayat et al. [11]	**Present Study**
0.1	1.1	0.1	0.74084	**0.73964**
0.3	1.1	0.1	0.70977	**0.69980**
0.5	1.1	0.1	0.68279	**0.66021**
0.1	1.2	0.1	0.74410	**0.75010**
0.1	1.3	0.1	0.74775	**0.76025**
0.1	1.4	0.1	0.75180	**0.75179**
0.1	1.1	0.05	0.73328	**0.73404**
0.1	1.1	0.15	0.74802	**0.74208**
0.1	1.1	0.2	0.75482	**0.73922**

4. RESULTS AND DISCUSSION

The numerical computations are conducted for different values of the parameters that describe the flow characteristics in Al_20_3-water nanofluid and the results are illustrated graphically. A representative set of computational results are presented in Figs. 2a-9c. The thermo-physical properties of water and nanoparticles are shown in Table 3. The Comparison of present results with the results reported by Hayat *et al.* [11] is made and found good agreement which is shown in Table 2.

Figs2a-2c exhibit the variation of f',g,θ with Grashof number(G).An increase in G enhances the primary velocity and reduces the secondary velocity in Al_20_3-nanofluid in the flow region.The temperature depreciate with increasing values of G.This is due to the fact that increase in G decays the thickness of the thermal and solutal boundaries.It is observed that the velocity profiles f ′ and g are both depreciates as the values of M increases in the boundary layer regimeinAl_2O_3-water nanofluid.This is due to the fact that the presence of magnetic field in the flow creates a force known as the Lorentz force which acts as a retarding force as a result the momentum boundary layer thickness decelerates throughout the flow region (Figs. 2a&b). The temperature graphs upsurge as the values of magnetic parameter increases (Fig. 2c)in Al_20_3-water nanofluid. This is because of the fact that to overcome the drag force imposed by the Lorentzian retardation the fluid has to perform extra work, this supplementary work can be converted into thermal energy which increases the thickness of the thermal boundary layer.

Figs.3a-3cexhibitf',g,θ with porous parameter (K) and viscosity parameter(B).From the profiles we find that lesser the permeability of the porous medium smaller the velocities in Al_20_3-water nanofluid in the flow region.The temperature grow with increasing values of K(figs.3c&d).This may be due to the fact that increase in K leads to thickening of thermal and solutal boundary layers. As the values of viscosity ratio parameter (B)increases the velocity profiles of f'elevates and graphs of g decelerates in based nanofluid region. It is seen from Fig.3c that the thickness of thermal boundary layer grows with higher values of(B).

An increase in slip parameter (B1) reduces the primary and secondary velocity and temperature in Al_2O_3-water nanofluid (figs.4a-4c).The velocity profiles of f ′ are reduced and that of g in based nanofluid are elevated as the values of velocity slip parameter (R1) increases in the boundary layer regime as shown in Fig. 4a&b.However the thermal boundary layer thickness in based nanofluid decay as the values of(R1) rises and is shown in Fig. 4c.

It is observed from Fig.5a&b that as the values of suction parameter(fw) increases both velocity profiles in Al_20_3-water nanofluid depreciate. This is due to the fact that suction is taken away the warm fluid from the surface of the sheet and thereby decreases the thickness of the velocity boundary layer. It is seen from Fig. 5c .that the thickness of thermal

boundary layer becomes thinner with higher values of fw(>0)while in the case of injection(fw<0) we find a decay in primary velocity and reduction in secondary velocity,temperaturein the fluid region.

The variation of velocities,temperature with heat transfer parameters(A11,B11) is shown in figs-6a-6c.From the profiles we find that the velocities and temperature experience enhancement with rising values of space/temperature dependent heat sources in the fluid region.

Figs.7a-7c depict the velocities, temperature profiles for different values of nanoparticle volume fraction (ϕ).It is perceived from Fig. 7a&7b.that primary velocity profiles f' upsurge and secondary velocity(g) diminishes in Al_20_3-water nanofluid as the nanoparticle volume fraction (ϕ) increases. This is due to the fact that increasing the nanoparticle volume fraction enhances the momentum boundary layer thickness in the flow region. It is noticed from Fig. 7c, the temperature profiles retard as the nanoparticle volume fraction increases. This is due to the fact that as ϕ increases the thickness of thermal boundary layers become thinner in the flow region.An increase in Prandtl number(Pr) produces a depreciation in the primary velocity,temperature and an enhancement in the secondary velocityin the flow region.Pr is the ratio of the rate of viscous diffusion to the rate of thermal diffusion,increased values of Pr corresponds to reduction in the thermal diffusivity which leads to the decreasing of energy ability resulting in the shrinking of the thermal boundary layer.

An increase radiation parameter (Rd) raises velocity profiles f′and g increases in based nanofluid region and is shown in Fig.8a&b. It is perceived from Fig.8c that as the values of Rd increases the temperatureprofiles are decay in the flow region. This is because of the fact that the mean absorption coefficient decreases with increasing values of radiation parameter; as a result the thermal boundary layer thickness of the fluid decay.Also an increase in the temperature difference ratio parameter(A) leads to a depreciation in both velocities,temperature in the flow region.This may be due to the fact that with increase in temperature ratio(A) the momentum,thermal boundary layer thickness become thinner(8a-8c).

Figs.9a-9c represent the effect of Forchheimer parameter(fs) on f',g and θ.An increase in fs depreciates primary velocity and upsurge secondary velocity,temperature in the entire flow region.Thus the inclusion of non-Darcy term in the momentum equations leads to decay in primary velocity and growth in secondary velocity,temperature.

Table.3 exhibits the variation of skin friction(τx, τz),Nusselt number(Nu) on η=0 for different parametric variations.An increase in Grashof number grows the skin friction coefficient τx,τz. Nu on the wall in Al_20_3-water nanofluid.Higher Lorentz force/lesser theporous permeability larger τx,τz,smaller Nu on η=0 in Al_20_3-water nanofluid.Higher the viscosity parameter(B)/temperature difference ratio parameter(A)smaller skin friction τx,larger τz and Nusselt number at η=0.Higher radiative heat flux/Prandtl number(Pr) smaller the skin friction coefficients.Nu reduces with Rd and enhances with Pr on the wall.Higher viscosity parameter(B) smaller τx,Sh, larger τz and Nu in Al_20_3-water nanofluid.An increase in nanoparticle volume fraction(ϕ) reduces τz and enhances τx,Nu on the wall.The skinfriction coefficients reduces with slip parameter(B1) and enhances with increase in R.Nu reduces with B1 and grow with R on the wall.τx,τz,Nu grow with increase in suction parameter(fw>0) while an increase in injection parameter(fw<0)grows τx,decays τz,Nu on η=0.With rising values of Space/temperature dependent (A11,B11) the skin friction components and rate of heat transfer grows on the wall η=0. Higher Forchheimer parameter(fs) larger the skin friction τ_z and rate of heat transfer (Nu), smaller τ_y on η=0. Thus the inclusion non-Darcy term in the momentum eq. leads to an enhancement in τ and Nu.

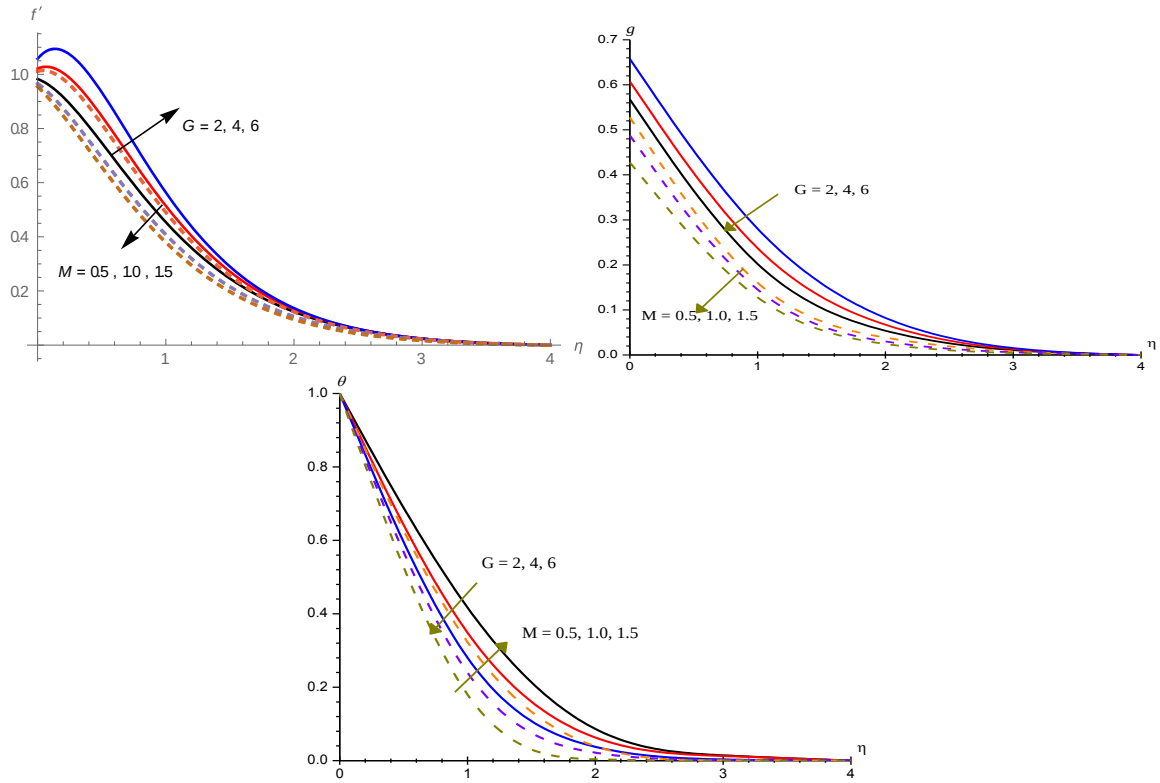

Fig.2.Variation of [a] axial velocity(f′), [b] secondary velocity(g), [c] temperature(θ) with G and M
K=0.2,B=0.5, B1=0.1,R1=0.1,fw=0.1, ϕ=0.05,Pr=6.20, Rd=0.5, A=1.05, fs=0.1, A11=0.1, B11=0.1

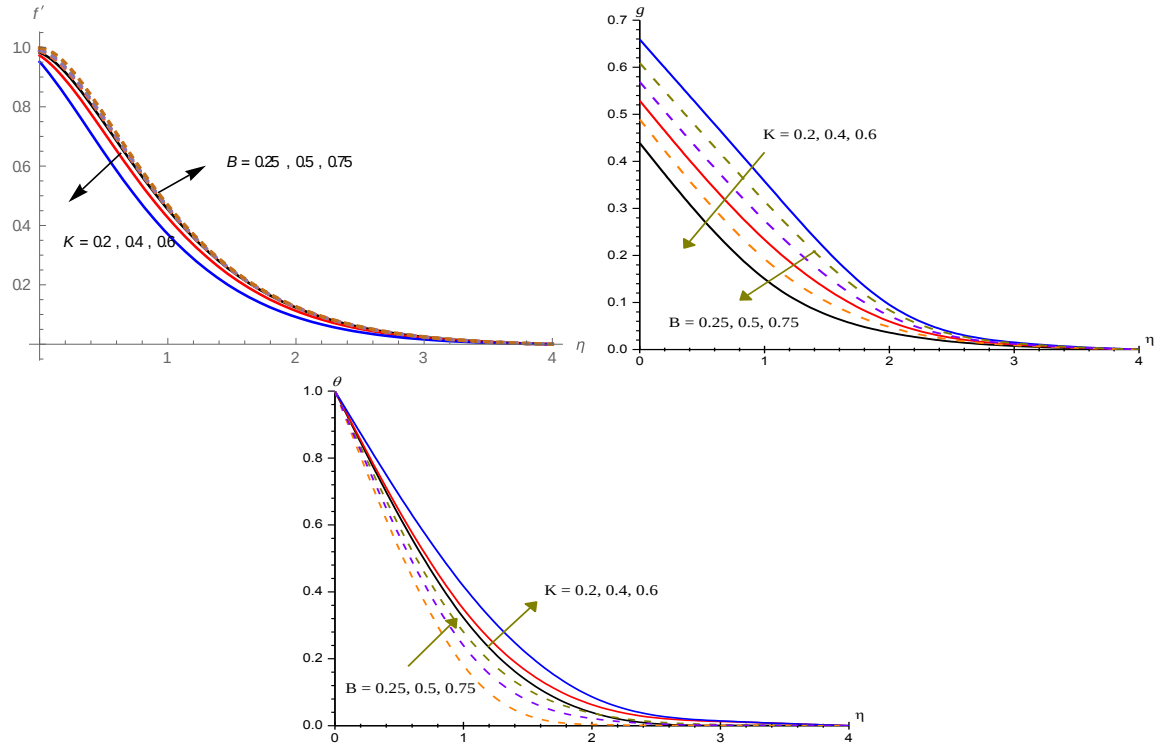

Fig.3.Variation of [a] axial velocity(f′), [b] secondary velocity(g), [c] temperature(θ) with K and B
G=2, M=0.5, B=0.1,R1=0.1,fw=0.1, ϕ=0.05,Pr=6.20, Rd=0.5, A=1.05, fs=0.1, A11=0.1, B11=0.1

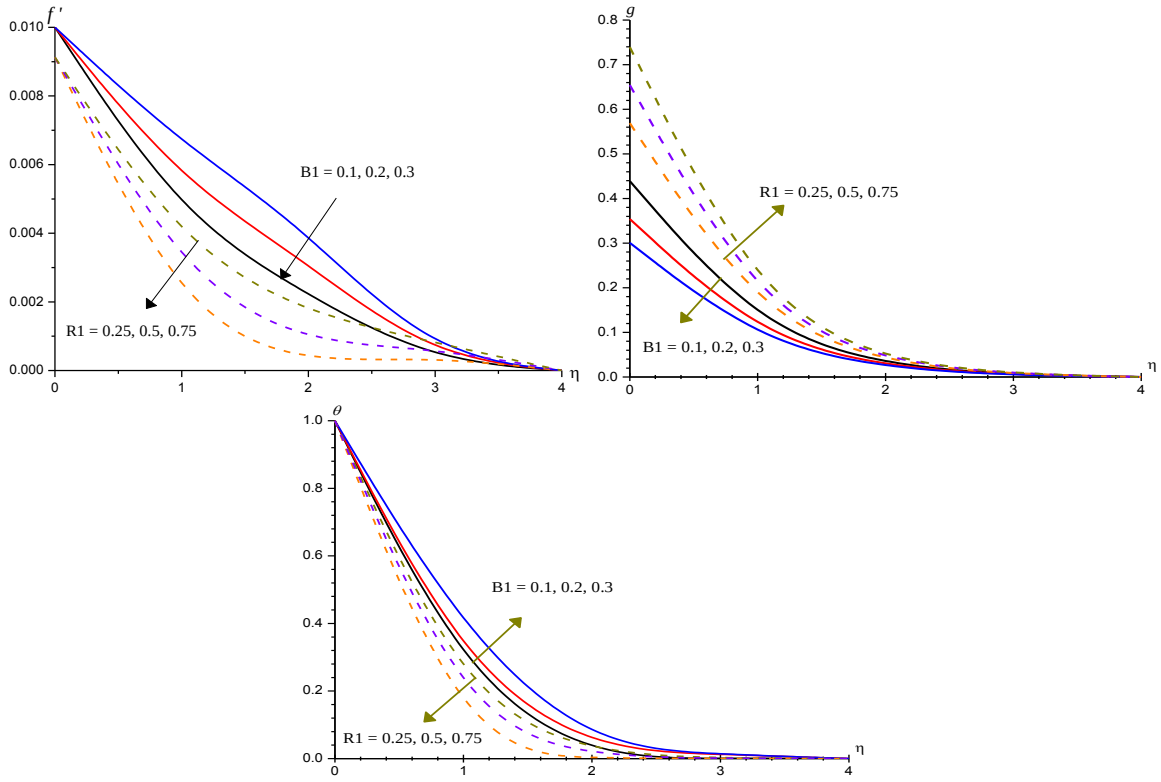

Fig.4.Variation of [a] axial velocity(f′), [b] secondary velocity(g), [c] temperature(θ) with B1 and R1
G=2, M=0.5, K=0.2,B=0.5, fw=0.1, ϕ=0.05,Pr=6.20, Rd=0.5, A=1.05, fs=0.1, A11=0.1, B11=0.1

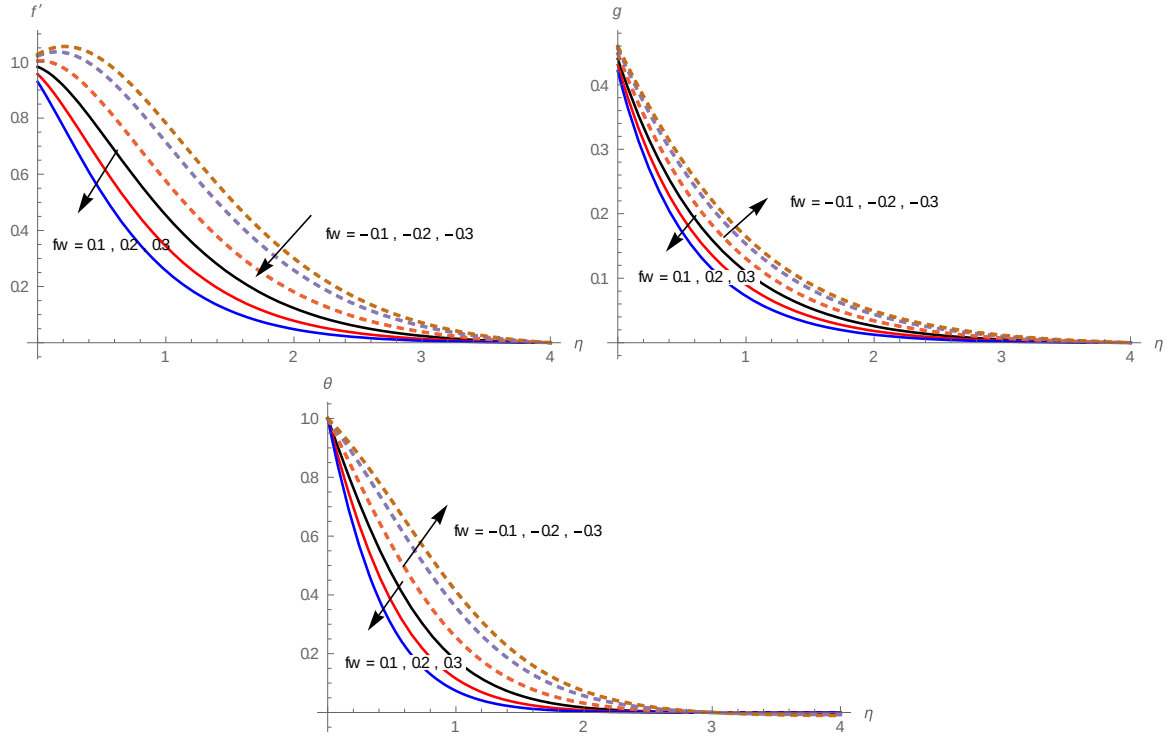

Fig.5.Variation of [a] axial velocity(f′), [b] secondary velocity(g), [c] temperature(θ) with fw
G=2, M=0.5, K=0.2,B=0.5, B1=0.1,R1=0.1, ϕ=0.05,Pr=6.20, Rd=0.5, A=1.05, fs=0.1, A11=0.1, B11=0.1

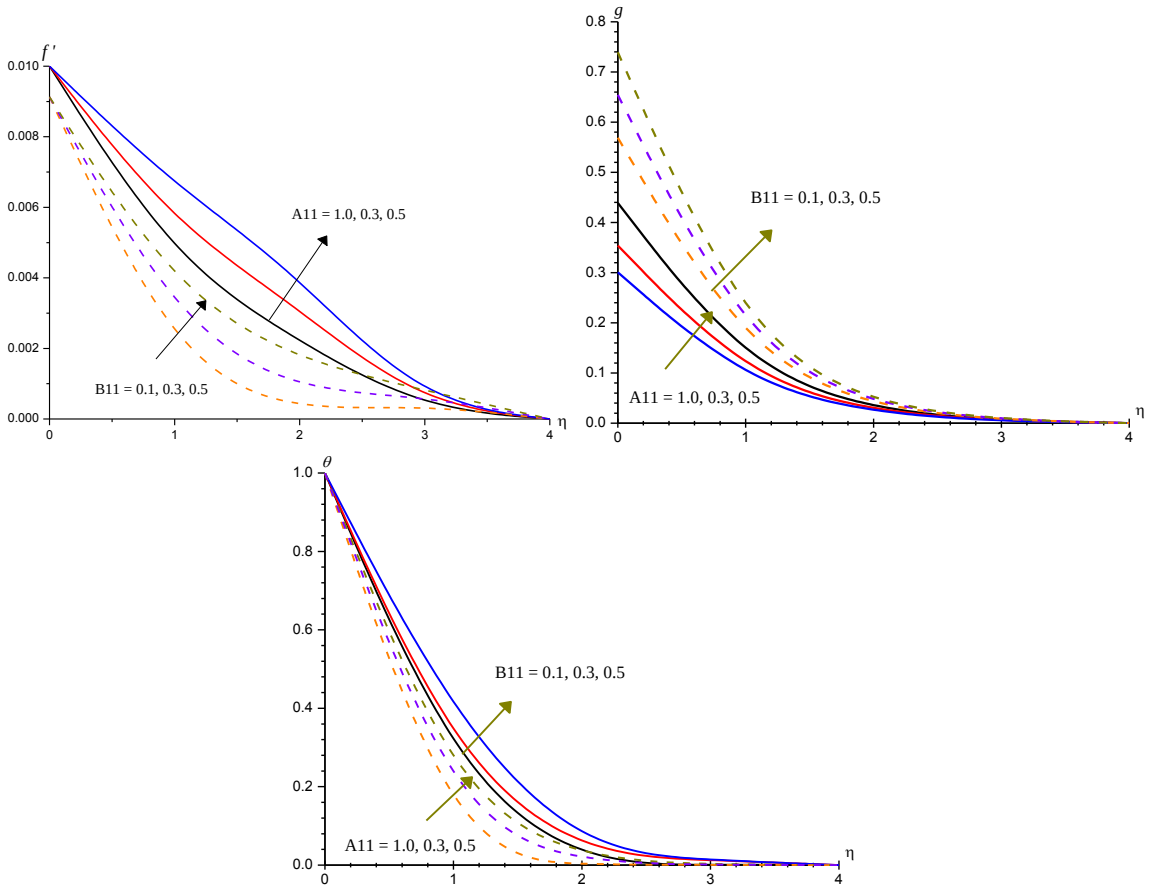

Fig.6.Variation of [a] axial velocity(f′), [b] secondary velocity(g), [c] temperature(θ) with A11 and B11
G=2, M=0.5, K=0.2,B=0.5, B1=0.1,R1=0.1,fw=0.1, ϕ=0.05,Pr=6.20

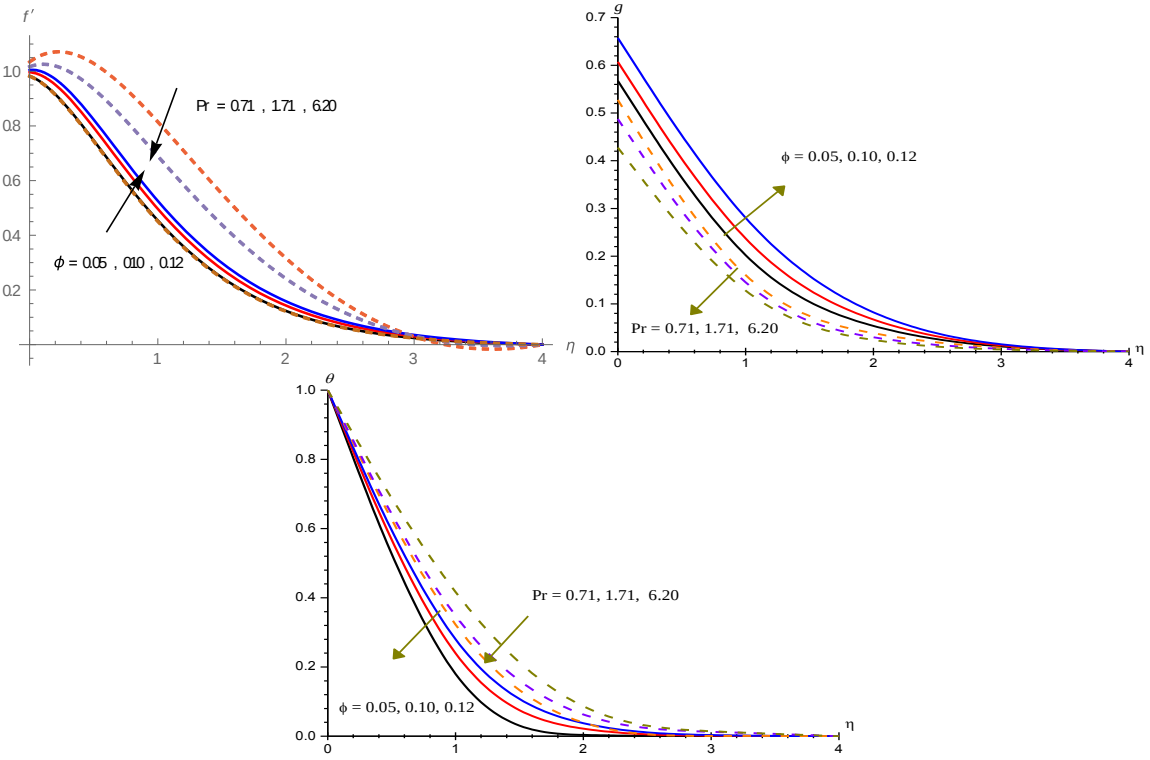

Fig.7.Variation of [a] axial velocity(f′), [b] secondary velocity(g), [c] temperature(θ) with ϕ and Pr
G=2, M=0.5, K=0.2,B=0.5, B1=0.1,R1=0.1,fw=0.1, Rd=0.5, A=1.05, fs=0.1, A11=0.1, B11=0.1

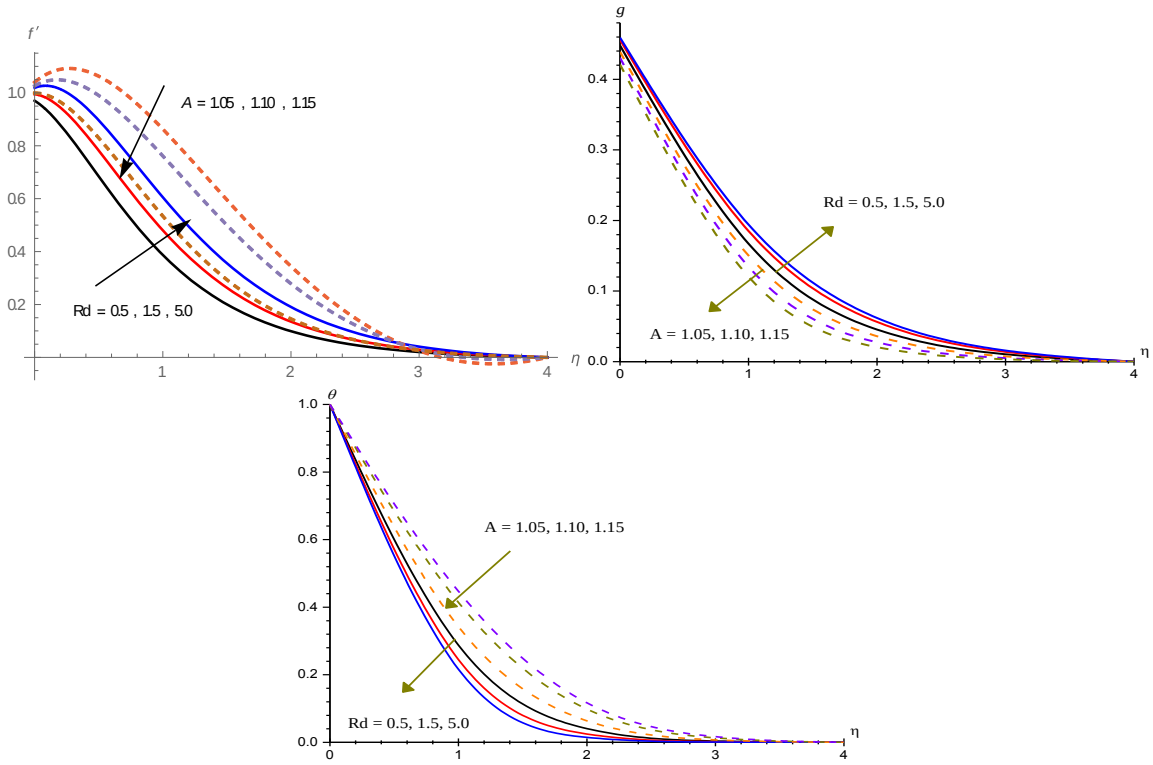

Fig.8.Variation of [a] axial velocity(f′), [b] secondary velocity(g), [c] temperature(θ) with Rd and A
G=2, M=0.5, K=0.2,B=0.5, B1=0.1,R1=0.1,fw=0.1, ϕ=0.05,Pr=6.20, fs=0.1, A11=0.1, B11=0.1

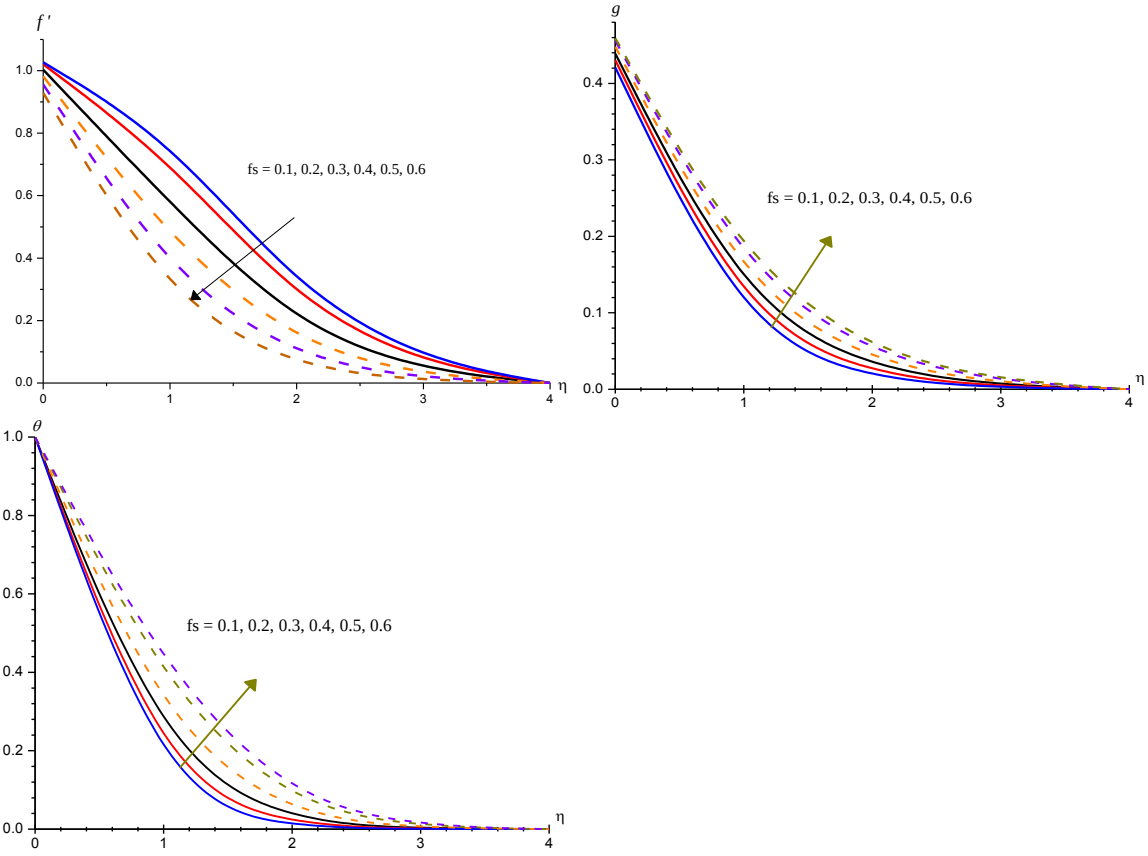

Fig.9.Variation of [a] axial velocity(f′), [b] secondary velocity(g), [c] temperature(θ) with fs
G=2, M=0.5, K=0.2,B=0.5, B1=0.1,R1=0.1,fw=0.1, ϕ=0.05,Pr=6.20, A11=0.1, B11=0.1

Table : 3 : Skin friction($\tau_{x,z}$), Nusselt number(Nu) at η=0

Parameter		Al_2O_3-water nanofluid			Parameter		Al_2O_3-water nanofluid		
		τx(0)	τz(0)	Nu(0)			τx(0)	τz(0)	Nu(0)
G	2	-0.173449	-0.601246	1.23976	B1	0.1	-0.173449	-0.601246	1.23976
	4	0.211555	-0.608177	1.28145		0.2	-0.115395	-0.469525	1.21018
	6	0.575444	-0.614439	1.31765		0.3	-0.085755	-0.390487	1.19225
M	0.5	0.119978	-0.646869	1.26407	R	0.2	-0.201526	-0.810487	1.27504
	1	-0.341282	-0.676058	1.20508		0.3	-0.219572	-0.956666	1.29778
	1.5	-0.453978	-0.724467	1.18195		0.5	-0.237125	-1.10681	1.31995
K	0.2	-0.173449	-0.601246	1.23976	ϕ	0.05	-0.0173449	-0.601246	1.23976
	0.4	-0.273251	-0.646174	1.21914		0.1	-0.0331084	-0.568093	1.27488
	0.6	-0.488846	-0.739206	1.17482		0.12	0.0475432	-0.54509	1.29433
B	0.5	-0.124192	-0.639771	1.23991	Pr	0.71	0.34485	-0.656044	0.436452
	0.75	-0.090335	-0.666247	1.24004		1.71	0.169965	-0.655312	0.597198
	1.0	-0.019732	-0.721446	1.24134		6.2	0.133932	-0.600291	1.254522
A	1.05	0.403654	-0.664471	0.35324	fw	0.1	-0.173449	-0.601246	1.23976
	1.15	0.267187	-0.670045	0.43588		0.2	-0.435159	-0.694886	1.68997
	1.20	-0.052994	-0.698405	0.74608		0.3	-0.708677	-0.790052	2.16893
Rd	0.5	-0.297744	-0.580753	1.53222		-0.1	0.037801	-0.519059	0.873125
	1.5	-0.206505	-0.565146	1.26578		-0.2	0.208237	-0.440794	0.563091
	5.0	0.190337	-0.564389	0.97633		-0.3	0.269172	-0.406597	0.443718
fs	0.1	-0.297744	-0.580753	1.53222	B11	0.1	-0.173449	-0.601246	1.23976
	0.2	-0.306504	-0.545130	1.26558		0.3	-0.191990	-0.769525	1.25018
	0.3	0.320336	-0.524387	0.97573		0.5	-0.225765	-0.990487	1.28425
	0.4	0.340336	-0.504387	0.99572					
A11	0.1	-0.297744	-0.580753	1.53222					
	0.3	-0.316503	-0. 651460	1.26692					
	0.5	0.350342	-0.674392	0.99628					

5. CONCLUSIONS

Three-dimensional flow heat transfer of Al_20_3 –water based nanofluid over porous stretching sheet with variation in viscosity is studied in this analysis. The primary velocity distribution elevates, secondary, temperature decelerate with the higher values of (ϕ) in Al_20_3-water nanofluid. It is worth to mention that the heat rate improve in Al_20_3-water as the values of ϕ increase. Increasing values of *M,K,B1* accelerates the temperature of the fluid.

The temperature rise with B1 and reduce with R on the wall. Primary velocity, temperature enhance, secondary velocity with viscosity parameter(B).Nu grows decays for higher values of viscosity parameter. Higher the strength of the space/temperature(A11/B11) dependent heat source leads to a depreciation in the flow variables. The inclusion of non-Darcy (Forchheimer (fs)) term in the momentum equations leads to decay in primary velocity and growth in secondary velocity, temperature.

6. REFERENCES

[1]. Ali ME. The effect of variable viscosity on mixed convection heat transfer along a verticalmoving surface. Int J Thermal Sci 2006:45:60-9.

[2]. Alivene B., Sreevani M. (2017): "Effect of Variable Viscosity, Radiation Absorption on Non-Darcy MHD Convective Heat and Mass Transfer Flow Past Stretching Sheet with Non-Uniform Heat Sources" *Chemical and Process Engineering Research*, Vol.47, p-12-20, 2017 ISSN 2224-7467 (Paper) ISSN 2225-0913 (Online), web : www.iiste.org

[3]. Animasaun I.L., Raju C.S.K., Sandeep N., Unequal diffusivities case of homogeneous–heterogeneous reactions within viscoelastic fluid flow in the presence of induced magnetic-field and nonlinear thermal radiation, Alexandr. Eng. J. (2016).

[4]. Bhatti MM, Rashidi MM. Effects of thermo-diffusion and thermal radiation on Williamson nanofluid over a porous shrinking/ stretching sheet. J Mol Liq. 2016; 21:567-73.

[5]. Buongiorno J. Convective transport in nanofluids. J Heat Transf. 2006; 128:240-50.
[6]. Choi SUS. Enhancing thermal conductivity of fluids with nanoparticles. In: Proceedings of the ASME international mechanical engineering congress and exposition, FED-vol. 231/MD-vol. 66; 1995, p. 99-105.
[7]. Cortell R., Fluid flow and radiative nonlinear heat transfer over a stretching sheet, J. King Saud Univ. – Sci. 26 (2) (2014) 161– 167.
[8]. Devasena Y: Effect of non-linear thermal radiation,activation energy on hydromagnetic convective heat and mass transfer flow of nanofluid in vertical channel with brownian motion and thermophoresis in the presence of irregular heat sources, *World Journal of Engineering Research and Technology* (JERT) *wjert, 2023, Vol. 9, Issue 2, XX-XX*, ISSN 2454-695X, SJIF Impact Factor: 5.924, www.wjert.org
[9]. Devi SPA, Prakash M. Temperature-dependent viscosity and thermal conductivity effects on hydromagnetic flow over a slendering stretching sheet. J of Nig Math Soc. 2015;34:318-330.
[10]. Ergun S. Fluid through packed columns. Chem. Eng. Prog. 1952;48:89-94.
[11]. Hayat T. T. Muhammad A. Alsaedi and M. S. Alhuthali Magnetohydrodynamic three-dimensional flow of visco-elastic nanofluid in the presence of nonlinear thermal radiation Journal of Magnetism and Magnetic Materials 385 pp.222-229 (2015).
[12]. Hussain S.T., Ul Haq R., Noor N.F.M., Nadeem S., Non-linear radiation effects in mixed convection stagnation point flow along a vertically stretching surface, Int. J. Chem. React. Eng. (2016).
[13]. Isaac LA, Anselm OO. Effects of variable viscosity, dufour, soret and thermal conductivity on free convective heat and mass transfer of non-Darcian flow past porous at surface. Amer J of Comp Math 2014;4:357-365.
[14]. Khan M.I., Haq F., Khan S.A., Hayatand T. Khan M.I., Development of thixotropic nanomaterial in fluid flow with gyrotactic microorganisms, activation energy, mixed convection. Computer Methods and Programs in Biomedicine, 187, (2019), 105186.
[15]. Khan M.I., Hayat T., Khan M.I. and Alsaedi A., Activation energy impact in nonlinear radiative stagnation point flow of Cross nanofluid. International Communications in Heat and Mass Transfer, 91, (2018), 216-24.
[16]. Khan WA, Pop I. Boundary-layer flow of a nanofluid past a stretching sheet. Int J Heat Mass Transf. 2010; 53:2477-83.
[17]. Krupalakshmi K.L., Gireesha B.J., Mahanthesh B., Gorla R.S.R., Influence of nonlinear thermal radiation and magnetic field on upper-convected Maxwell fluid flow due to a convectively heated stretching sheet in the presence of dust particles, Commun. Numer. Anal. 2 (2016) 1–18.
[18]. Mabood F., Nayak M.K. and Chamkha A.J., Heat transfer on the cross flow of micropolar fluids over a thin needle moving in a parallel stream influenced by binary chemical reaction and Arrhenius activation energy. The European Physical Journal Plus, 134(9), (2019), 427
[19]. Mahanthesh B, Gireesha BJ, Gorla RSR. Nonlinear radiative heat transfer in MHD three-dimensional flow of water based nanofluid over a non-linearly stretching sheet with convective boundary condition. J Niger Math Soc. 2016; 35:178-98.
[20]. Makinde O.D., Mabood F, Khan W.A., Tshehla M.S. : MHD flow of a variable viscosity nanofluid over a radially stretching convective surface with radiative heat, Journal of Molecular Liquids, 219, (2016), pp.624-630, www.elsevier.com/ locate/molliq, http://dx.doi.org/10.1016/j.molliq.2016.03.078
[21]. Mushtaq A., Mustafa M., Hayat T., Alsaedi A., Effects of thermal radiation on the stagnation-point flow of upperconvected Maxwell fluid over a stretching sheet, J. Aerosp. Eng. 27 (4) (2013) 04014015.
[22]. Nagasasikala M : Effect of activation energy on convective heat and mass transfer flow of dissipative nanofluid in vertical channel with Brownian motion and thermophoresis in the presence of irregular heat sources, *World Journal of Engineering Research and*

Technology (JERT) *wjert, 2023, Vol. 9, Issue 2, XX-XX,* ISSN 2454-695X, SJIF Impact Factor: 5.924, www.wjert.org

[23]. Pantokratoras A. Further results on the variable viscosity on flow and heat transfer to a continuous moving flat plate. Int. J. Eng. Sci. 2004;42:1891-1896.

[24]. Pantokratoras A., Fang T., Sakiadis flow with nonlinear Rosseland thermal radiation, Phys. Scr. 87 (1) (2012) 015703.

[25]. Prabavathi B Sudarsana Reddy P Bhuvana Vijaya R (2019): Three-dimensional Heat and Mass Transfer Flow Over a Stretching Sheet Filled with Al_2O_3-water Based Nanofluid with Heat Generation/Absorption, Journal of Nanofluids. Vol. 8, No.6, pp. 1355–1361, doi:10.1166/jon.2019.1686 (www.aspbs.com/jon)

[26]. Rashidi MM, Freidoonimehr N, Hosseini A, Beg OA, Hung TK. Homotopy simulation of nanofluid dynamics from a non-linearly stretching isothermal permeable sheet with transpiration. Meccanica. 2014; 49:469-82.

[27]. Salem AM. Variable viscosity and thermal conductivity effect on MHD flow and heat transfer in viscoelastic fluid over a stretching sheet. Phys. Lett A 2007;369:315-22.

[28]. Satya Narayana K and Ramakrishna G N : Effect of variable viscosity, activation energy and irregular heat sources on convective heat and mass transfer flow of nanofluid in a channel with brownian motion and thermophoresis, *World Journal of Engineering Research and Technology* (JERT) *wjert, 2023, Vol. 9, Issue 2, XX-XX,* ISSN 2454-695X, SJIF Impact Factor: 5.924, www.wjert.org

[29]. Seddeek MA. Effect of non-Darcian on forced convection heat transfer over a flat plate in a porous medium with temperature dependent viscosity. Int. Commun Heat Mass Transfer 2005:32:258-65.

[30]. Shehzad S.A., Hayat T., Alsaedi A., Obid M.A., Nonlinear thermal radiation in three-dimensional flow of Jeffrey nanofluid: a model for solar energy, Appl. Math. Comput. 248 (2014) 273– 286.

[31]. Sheikholeslami M, Rashidi MM, Ganji DD. Effect of non-uniform magnetic field on forced convection heat transfer of Fe_3O_4 water nanofluid. Comput Methods ApplMech Eng. 2015; 294:299-312.

[32]. Singh P, Tewani K. Non-Darcy free convection from vertical surface in thermally stratified porous medium. Int. J. Eng. Sci. 1993;31:1233-42.

[33]. Singh V, Shweta A. Flow and heat transfer of maxwell fluid with variable viscosity and thermal conductivity over an exponentially stretching sheet. Amer J of Fluid Dyn. 2013;3(4):87-95.

[34]. Sreenivasulu P, Poornima T, Bhaskar R. Variable thermal conductivity influence on hydromagnetic flow past a stretching cylinder in a thermally strati_ed medium with heat source/sink. Fron in Heat and Mass Trans. 2017;9(20):1-7.

[35]. Vajravelu K, Prasad KV, Chiu-on N. Unsteady convective boundary layer flow of a viscous fluid at a vertical surface with variable fluid properties. Nonl Analy: Real World Appl. 2013;14:455-464.

[36]. Wakif A, Boulahia Z, Ali F, Eid MR, Sehaqui R. Numerical analysis of the unsteady natural convection MHD Couettenanofluid flow in the presence of thermal radiation using single and two phase nanofluid models for Cu–water nanofluids. Int J ApplComput Math. 2018;4:81.

[37]. Wakif A, Boulahia Z, Amine A, Animasaun IL, Afridi MI, Qasimd M, Sehaqui R. Magneto-convection of alumina-water nanofluid within thin horizontal layers using the revised generalized Buongiorno's model. Front Heat Mass Transf (FHMT). 2019;12:3.